



A GNSS/UWB Integrated Positioning Methodology for Geo-Localization

Ngye Antoinette Agwa¹, Takumi Kobayashi², Chika Sugimoto³, Ryuji Kohno⁴

^{1,2,3}Graduate School of Engineering Science, Yokohama National University, Japan

⁴University of Oulu Research Institute Japan

Abstract— Global navigation satellite system (GNSS) is the most used relative positioning technology today for land surveys. However, this positioning method is not suitable for indoor or dense urban environments because the positioning accuracy is greatly affected by obstructions from tall buildings and trees that can cost the deviation of signals. On the other hand, Ultra-wideband (UWB) is a local positioning technology used for local measurements in a high multipath environment. This paper focuses on the integration methodology between GNSS and UWB (GNSS/UWB) for outdoor positioning based on Real-Time Kinematic (RTK). We equally proposed a method for anchor nodes positioning used to determine the target node coordinates. Simulation results with MATLAB showed that a survey based on GNSS/UWB was exceptionally efficient technology for the environment with very poor satellite visibilities and allowed for reliable millimeters accuracy. The coordinates of each point were obtained in less than 2 minutes of the observational sessions.

Index Terms— GNSS/UWB Integration, Cadastral Map, Digital Land Points, Localization Accuracy, Particle Filter and Geo-Localization

I. INTRODUCTION

CADASTRAL maps are certificate-having law forces held by the land creditor. It described the cadastral geographical location, boundary points, boundary lines, and the adjacent relationship between cadastral. Da Bing Yang, et. al. proposed that land mapping was a necessary complement of land certificates' records and addressed, the importance of handling land ownership certificates [1]. A method to improve the digital map's reliability and accuracy using GPS/INS-based low-order extended kalman filter (EKF) has been proposed. The accuracy of cadastral mapping is a critical technology in the establishment of a cadastral management system. Cadastral mapping is the combination of spatial data and attributes data. In practice, Static and Real-time Kinematic (RTK) positioning is used in GPS surveys. Artur Oruba, et. al. proposed a network of a reference system that enables the automatic processing of static data observed from any user, which reduces the minimum observation period to about 15min for line-of-sight [2]. Satellite observation methods require measurements to be carried out in an open area, which is a major limitation. When there is no direct path from the satellite to the receiver, the survey becomes difficult,

sometimes impossible, using traditional GNSS techniques [3]. The avoidance of GNSS measurements in the forest, a very dense urban and mountain environment is increasing due to poor localization. Previous research proposed precise point positioning technology [4], static surveying [5], [6], differential code measurement [7], method of absolute measurement [8], and RTK [9] to reduced positioning error in such environment; however, the positioning accuracy was poor. Mieczysław Bakula, et. al, analyses the accuracy conditions with limited visibility of satellites using three GPS/GLONASS receivers set up on a particular measurement beam [10]. However, many visible satellites are observable for multi-GNSS positioning, which becomes very cumbersome to mitigate. A method of satellite selection was proposed in [11] to minimize this effect. The primary source of high-accuracy field surveys is (challenging to eliminate) the multipath error [12]. Multipath is the recording of reflected signals by the GNSS receiver. This signal reflection can be of two types. It can reflect the ground that arrived at the receiver's antenna [13] or obstacle standing near the receiver (trees, mountain, tall buildings). The satellite movement and the orbit cost continually satellite geometry change; the multipath impact level depends on the altitude of a given satellite and time. Signals high in the zenith are of less risk to multipath effect compared to low satellites. [14] proposed that at reference stations, measurements can be done in 15-30min cycles in other to minimized multipath error. The required observation time is a disadvantage. In kinematic and rapid static GNSS surveys, the multipart effect was considered the primary source of error [15] and increased observation time to several minutes. [16] proposed that the multipath effect can be minimized using several receivers.

In dense urban, mountain, forest, and indoor environments, precise positioning has always been a more challenging problem for many reasons. The GNSS signal is not strong enough to penetrate most materials. As soon as an object hides the GNSS satellite from the target's view, the signal is corrupted, limiting GNSS's usefulness to open environments and limiting its performance in the mountains, dense urban, and forest environments, as retaining a lock on the GNSS signals becomes very difficult. GNSS typically becomes almost useless in such challenging environments. However,

there is an increasing need for precise localization in cluttered environments, in addition to open spaces. For example, in a land survey, accurate localization of digital land points is an emerging need, “blue force tracking” that knows where friendly force is, is of great significance, must especially in urban scenarios. A promising solution to minimize the multipath effect and increase position accuracy is radio signals like UWB technology because UWB ranging has several characteristics, which give them superiority over GNSS signals in low to limited signal environments. UWB’s sufficient time resolution ability, high-speed data transmission, accurate position estimation, low power transceiver designs, and robust performance in dense multipath environments can improve the GNSS navigation system. Furthermore, UWB ranging provides the capability to augment GNSS through high accuracy ranges. UWB information is transmitted through a series of baseband pulses instead of the modulated sinusoidal carrier in an impulse signal. On the other hand, multi-carrier UWB signals use a set of sub-carriers. Each of these sub-carriers must not interfere with one another and should overlap. The ability of multi-carrier UWB signals to minimize interference with bands used by different systems sharing the spectrum is advantageous [17]. UWB gives significant advantages in numerous applications, including industrial RF monitoring systems, high-speed LAN, Unmanned Aerial vehicles (UAV), Intrusion Detection Radars, and Unmanned Ground vehicles (UGV) precise positioning, Tactical Handheld Radios, and more. Other additional advantages of UWB include;

- 1) *With power spread over huge bandwidth, frequency selective fading from multipath/materials is mitigated [18].*
- 2) *Ranging – very fine precision distance and range resolution.*
- 3) *Low energy density gives less interference to closer systems and minimal RF health hazards.*
- 4) *Minimal multipath cancellation effects.*

Multipath nullification happens when a multipath signal arrives at the anchor node partially or totally out of phase with the direct signal. It causes a reduced amplitude response. With a short period of signal pulses, direct signals will arrive before indirect signals. As a result, they are fewer multipath cancellation effects with UWB signals. UWB, like GNSS technology, is still subject to physics laws for radio frequency signals such as trade-off versus bandwidth. Another issue with UWB is its ranging accuracy. In addition, UWB provides reliable and precise results regarding relative positioning concerning a local frame, at the cost of covering the working area with expensive antennas, thereby limiting UWB technology only to a relatively small extent outdoor and applicable indoor. On the other hand, GNSS is a cheap technology that offers an adequately accurate localization outdoor worldwide, in terms of a global frame (longitude, altitude, latitude). Using UWB to increase GNSS enlarges navigating and positioning in areas where GNSS typical falters; this is mostly indoors or in hostile signal environments. Because both systems are harmonious, integrating these sensors for precise positioning draws benefits from both types of sensors while reducing their drawbacks. Previous sensor fusion proposed that a particle filter can

combine GPS/UWB for and out/indoor scenarios, but there were no descriptions on anchor node placement. Besides, GPS provides low accuracy when compared to GNSS technology [19]. [20] equally shown that they were improvement in combining UWB and GPS. However, precision is also a function of the UWB beacon’s location; besides, the estimation was slightly sensitive to the location’s initial guess. Finally, [21] uses a single UWB range to increase GPS in hostile environments. The analysis shows a rapid convergence of the Kalman filter positioning and reduced Dilution of Precision (DOP) values with the UWB range’s augmentation. The goal of this research work can be summarized as follow:

- 1) *Show that an integrated GNSS-UWB solution is more accurate and reliable than a GNSS-only solution under conditions with limited access to satellite signals.*
- 2) *Show that the accuracy depends on anchor node positioning.*
- 3) *Show a reduction in observation time.*

This paper focuses on the probabilistic combination of sensor data acquired from different sources; GNSS global and a local positioning technique like UWB. More precisely, we propose a Monte Carlo (Particle Filter) localization algorithm, representing the target node’s position poses using a set of weighted samples (particles). As an advantage, this approaches ability to combine measurements from different sensors while considering their probabilistic behaviors appropriately.

II. PRELIMINARIES

A) Analysis of GNSS/UWB

UWB provides better accuracy than GNSS, both indoor and outdoor; however, it can only offer local coordinates of a point. On the contrary, GNSS provides relative coordinates. A tightly coupled GPS/Wi-Fi integration was proposed in [22] to address GPS outages and improve the overall positioning accuracy to about 2.75m. [19] uses a particle filter to fuse GPS and UWB measurements in an indoor/outdoor track. Although UWB measurements are intermittent outdoor, they are still improving positioning accuracy when the measures are integrated. In the proposal, comparisons were made when the robot only relies on the odometric system for its position, and the robot position is estimated using a particle filter while considering UWB range measurements. When the GPS signal is available, they were combined to improve robot localization with about 37cm accuracy.

In our proposer, we used UWB/GNSS signal to provide better accuracy for digital land points since latitude and longitude are required to locate a point on the earth’s surface, as presented in Fig. 1. We assume that all anchor nodes (ANs) are involved in the positioning and that the target coordinates are the same as the vertex. For each AN, the input information includes each GNSS measurement at the integration time with the target. It is equally considered that GNSS clock error is minimized [23] by using additional satellites to correct anchor nodes to satellites clock error. Localization can be achieved by self-positioning (target nodes estimated its position or by remote-positioning (central unit which calculates position

information from different anchor nodes) [24]. This work's positioning technique is remote positioning combined with a two-step positioning system that uses TDOA localization techniques due to its low complexity compared to direct positioning, whose position is estimated directly from its received signal [25], [26]. In [27], it was proven that ToA is commonly preferable for the UWB position; combining ToA/TDOA gives more accurate results. *GNSS Positioning Equation*

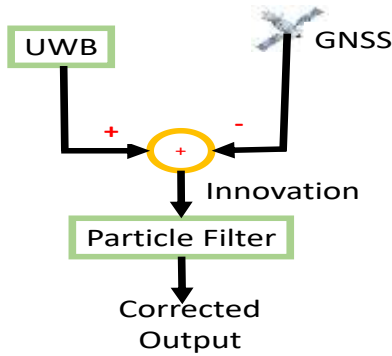


Fig. 1. GPS Aided UWB Sensor Fusion

The GNSS pseudo-range observation equation is given by

$$p_{i,j} = R_{i,j} + c(\hat{\partial}t_u - \hat{\partial}t^{sat}_{i,j}) + \varepsilon_{i,j} + I_{i,j} + T_{i,j} \quad (1)$$

where $\hat{\partial}t_u$ is the receiver clock offset, $\hat{\partial}t^{sat}_{i,j}$ is the satellite clock offset, $I_{i,j}$ is the Ionospheric error, $T_{i,j}$ is the tropospheric error, $\varepsilon_{i,j}$ is the measurement noise and c is the speed of light.

The observation equation from m^{th} satellite to receiver can be written as;

$$R_{i,l} = \sqrt{(x^{sat}_{i,j} - x_u)^2 + (y^{sat}_{i,j} - y_u)^2 + (z^{sat}_{i,j} - z_u)^2} \quad (2)$$

$$+ \omega_e (x^{sat}_{i,j} y_u - y^{sat}_{i,j} x_u) / c$$

$$= \|X^{sat}_{i,j} - X_u\| + \varphi_e \nu$$

where $X_{i,j}^{sat} = [x_{i,j}^{sat}, y_{i,j}^{sat}, z_{i,j}^{sat}]^T$,

$X_u = [X_u, Y_u, Z_u]^T$ and φ_e is the angular velocity of earth rotation (m/s) Equation (1) can be represented in vector form as:

$$\rho_{i,j} = \|X^{sat}_{i,j} - X_u\| + \varepsilon_{i,l} + I_{i,j} + T_{i,j} \quad (3)$$

With the availability of multi-GNSS in the sky, a grant number of the satellite can be observed simultaneously, with some having very bad GDOP. Therefore, it becomes vital to select satellites having good GDOP. The absolute value of residual ranging error can be used as an evaluation method to determine satellites with good GDOP, as proposed in [11].

$$\rho_{i,j} = |p_{i,j} - p^*_{i,j}| \quad (4)$$

$$\rho^*_{i,j} = R^*_{i,j} + c(\delta^* t_u - \delta^* t^{sat}_{i,j} + \delta^* t_{syn}) + I^*_{i,j} + T^*_{i,j} \cdot R^*_{i,j}$$

Where $\delta^* t_{syn}, \delta^* t_u$ are the estimated values from all visible satellites and $\delta^* t_{i,l}, T^*_{i,j}, I^*_{i,j}$ are the broadcast ephemeris correct values. The residual ranging error includes ephemeris error, satellite vehicle clock error, positioning error, multipath effect, modeling of the ionosphere and troposphere error, and measurement noise. The positioning accuracy becomes worse if the measurement value of residual ranging error is high. Therefore, if the residual range error meets equation (5), then it should be eliminated.

$$\rho_{i,j} \Rightarrow \alpha + 2\kappa \quad (5)$$

where $\alpha, 2\kappa$ are the standard deviation (STD) and average residual ranging errors respectively.

The position state \mathbf{x} is in rectangular coordinates so, these coordinates have to be converted from Cartesian to Geodetic coordinates as follows:

$$\begin{bmatrix} x \\ y \\ z \end{bmatrix} = \begin{bmatrix} (F_r + h) \cos \beta \cos \lambda \\ (F_r + h) \cos \beta \sin \lambda \\ \{F_r (1 - e^2) + h\} \sin \beta \end{bmatrix} \quad (6)$$

Where (F_r) is the Earth's ellipsoid meridian radius of curvature, and Meridian ellipse eccentricity is e . Therefore, we can deduce the GPS estimated position as represented in (7) at the top of the next page.

B) UWB Positioning

In order to compute the user position a minimum of three UWB reference nodes are required for UWB TDOA-based positioning. According to [28] the actual range equation of UWB is given by

$$\rho^w_{i,j} = \theta_{i,j} + \mathcal{G}_{i,j} + \xi^w_{i,j} \quad (8)$$

Where $\theta_{i,j}$ is the range estimation error, $\mathcal{G}_{i,j}$ is the TDOA estimation at reference node i , and $\xi^w_{i,j}$ is the pseudorange measurements.

$$\xi^w_{i,j} = \sqrt{(x^w_{i,j} - x_{sat})^2 + (y^w_{i,j} - y_{sat})^2 + (z^w_{i,j} - z_{sat})^2} \quad (9)$$

$$= \|X^w_{i,j} - X_{sat}\| + \varphi^w_e$$

where, φ^w_e is UWB positioning error, $x^w_{i,l}, y^w_{i,j}, z^w_{i,j}$ are the coordinates of the i^{th} UWB reference node, and $x_{sat}, y_{sat}, z_{sat}$ are the satellite coordinate. Repeating steps in section 2.2, we can deduce UWB estimated position as in (10).

B) Particle Filter

This is a recursive filtering algorithm use in handling non-linear and non-Gaussian parameter and system state estimation. We employ a Particle Filter because the probabilistic observation model of UWB sensors is non-linear. Also, it leads to distributions that can be difficult to approximate by Gaussian, and PF is good for arbitrary

distributions, which enable global localization of anchor nodes at start-up. [29], [30], [31] presented the particle filter algorithm principle as a non-parametric form of Bayes filter. The state-space generates random samples in groups that depend on the posterior conditional for distributing the system state vector. The particle's position and weight are adjusted continuously [32] based on its measured value until the convergence of state quantity.

$$\xi_G^{(i,j)} \begin{bmatrix} r_c^1 \\ \cdot \\ \cdot \\ r_c^{Gn} \end{bmatrix} = \begin{bmatrix} \sqrt{\left((F_r + h)\cos\varphi\cos\lambda - x_{i,j}^1\right)^2 + \left((F_r + h)\cos\varphi\sin\lambda - y_{i,j}^1\right)^2 + \left((F_r + h)\sin\varphi - z_{i,j}^1\right)^2} + \alpha_r + \varepsilon_p^1 \\ \cdot \\ \cdot \\ \sqrt{\left((F_r + h)\cos\varphi\cos\lambda - x_{i,j}^G\right)^2 + \left((F_r + h)\cos\varphi\sin\lambda - y_{i,j}^G\right)^2 + \left((F_r + h)\sin\varphi - z_{i,j}^G\right)^2} + \alpha_r + \varepsilon_p^G \end{bmatrix} \quad (7)$$

$$\xi_w^{(i,j)} \begin{bmatrix} r_c^1 \\ \cdot \\ \cdot \\ r_c^{wn} \end{bmatrix} = \begin{bmatrix} \sqrt{\left((F_r + h)\cos\varphi\cos\lambda - x_{i,j}^1\right)^2 + \left((F_r + h)\cos\varphi\sin\lambda - y_{i,j}^1\right)^2 + \left((F_r + h)\sin\varphi - z_{i,j}^1\right)^2} + \alpha_r + \varepsilon_p^1 \\ \cdot \\ \cdot \\ \sqrt{\left((F_r + h)\cos\varphi\cos\lambda - x_{i,j}^w\right)^2 + \left((F_r + h)\cos\varphi\sin\lambda - y_{i,j}^w\right)^2 + \left((F_r + h)\sin\varphi - z_{i,j}^w\right)^2} + \alpha_r + \varepsilon_p^w \end{bmatrix} \quad (10)$$

PFs are suitable to work with almost random sensor characteristics, noise distributions, even non-linearities, and motion dynamics if and only if some likelihood model of their uncertainty can be given. They can simultaneously sustain different hypotheses about the pose of a target node. This ability permits the localization system to track a target node within complex and self-similar scenarios. As particle filters sample the space of possible positions up to a given sampling density, their computational cost can be limited, and they are easy to implement.

III. INTEGRATED GNSS/UWB POSITIONING USING PARTICLE FILTER

A) System Model

We consider a set of anchor nodes (UWB radios mount on a GNSS receiver) position, as presented in fig. 2 and with an embedded processor for particle filter processing. These anchor nodes use TDOA to measure the mobile handset position. The land surveyor moves from one point to another, collecting digital land points.

1) We derive the equations of our particle filter. Let z_t, v_t, x_t denote the observation for any given time step t , mobile user action and system state respectively. However, we are interested in the target pose. Unknown biases are used to augment the system state b_{k-1}^N of each UWB beacon, where N is the set of beacons that determine the 3D position b_k^N . Knowing that s_t evolves as a Markov chain, we can write our estimation problem as:

$$\begin{aligned} \rho &= (s_t | v_{1:t}, z_{1:t}) \propto \rho(z_t | s_t, v_{1:t}, z_{1:t-1}) \rho(s_t | v_{1:t}, z_{1:t-1}) \\ &= \underbrace{\rho(z_t | s_t)}_{\text{Observation model}} \underbrace{\int \rho(s_t | s_{t-1}, v_t) \rho(s_{t-1} | v_{1:t-1}, z_{1:t-1})}_{\text{Evolution model}} \end{aligned} \quad (11)$$

2) Considering that samples are drawn from the system transition such that;

$$q(z_t | s_{t-1}, v_t, z_t) = \rho(s_t | s_{t-1}, v_t) \quad (12)$$

Then, the important weight can be updated as:

$$\omega_t^i \propto \omega_{t-1}^{\{i\}} \rho(z_t | s_t^{\{i\}}) \quad (13)$$

3) We consider that the observation z_t contains GNSS reading and UWB range reading at a time step t . The observation variables can be defined as:

$$z_t \left(z_t^{GNSS,1}, \dots, z_t^{GNSS}, z_t^{UWB,1}, \dots, z_t^{UWB,M} \right) \quad (14)$$

4) Considering that the random errors of each of the measurements are independent, the observation likelihood can be summarized as:

$$\rho(z_t | s_t) = \prod_{k=1}^N \rho(z_t^{GNSS} | s_t) \prod_{k=1}^N \rho(z_t^{UWB,k,t} | s_t) \quad (15)$$

5) A Gaussian distribution obtained from GNSS satellites can appropriately model the position of each UWB as follows:

$$\rho(z_t^{GNSS} | s_t^{(i)}) = N\left(\xi^{(i)w}_t, z_t^{GNSS}, \Sigma_t^{GNSS}\right) \quad (17)$$

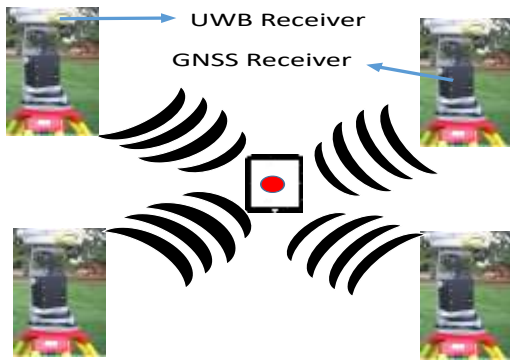


Fig. 2. Live View of GNSS/UWB Surveying Based on our Proposed Method.

Where \sum_t^{GNSS} is the number of satellites observed at each instant (t) and $\xi_i^{(i)w}$ is the position of each UWB.

6) The sensor model is accountable for the Gaussian noise only because the bias $b_{k,t}^{(i)}$ is jointly estimated to the system state as:

$$\rho(z_{k,t}^{UWB} | s_t^{(i)}) = N(X + b_{k,t}^{(i)}, z_{k,t}^{UWB}, \varepsilon^2_{UWB}) \quad (18)$$

Where X is the target position and ε^2_{UWB} is the positioning error.

7) Denote $N^{(i)}$ as the set of ANs of the target, $M^{(i)}$ as the number of visible satellites, and k is the GNSS output time. We now formulate the integrated positioning as follows:

- a) Find the posterior target distribution having state X_k with the information collected by GNSS/UWB as shown in (19)

$$\psi(X_k) = \rho(X_k | \zeta_{1:k}), \forall_i \in M \quad (19)$$

Where ψ is the collected information at corresponding time, $\zeta_k^{(i)}$ includes the GNSS and UWB measurement of AN, $i(\zeta_{G,k}^{(i)})$ and $\xi_{w,k}^{(i)}$, respectively.

8) Then, the X_k which makes a maximum with $\psi(X_k)$ is the integrated position $\psi(X_k)$ can be expressed as

$$\psi(X_k) = \int \rho(X_k | \zeta_{1:k}) \rho(X_k) \propto \underbrace{\rho(\xi_{G,k}^{(i)}, X_{k-1}, \xi_{w,k}^{(i)} | X_k)}_{\text{Likelihood of information}} \underbrace{\rho(X_k | X_{k-1})}_{\text{Prediction}} \psi(X_k) \quad (20)$$

B) Anchor Node Positioning

To guarantee that the target well gets continuous accuracy positioning, we must ensure that the target should not move out of range. A maximum number of ANs are placed such that the distance between the target and ANs is not greater than parameter λ_{\max} . We start by defining some useful notations.

TABLE I
SOME USEFUL NOTATIONS

TG	is the target
λ_{\max}	the maximal spacing constraint
$TG = (x_u, y_u, z_u)$	the location of target TG
$b = (x_c, y_c, z_c)$	the location of AN
b_*	the number of AN
A	is the coverage area

Anchor nodes placement can be represented as a coverage area, such that $g = L_1 \cup L_2, A$, where

$$L_1 = TG, L_2 = b. (TG, L) \in A, \Leftrightarrow \exists TG = (x_u, y_u, z_u),$$

such that $c = (x_c, y_c, z_c) \in b$, and

$$\sqrt{(x_u - x_c)^2 + (y_u - y_c)^2 + (z_u - z_c)^2} \leq \lambda_{\max}$$
 as shown

in Fig. 3 arrangement 2. In [28], it was proven by computer simulation that an increase in the distance from one AN to another reduces positioning error why closer ANs further increases the positioning error. Considering this critical fact, we proposed a GNSS/UWB error model base on the Dilution of Precision (DoP) technique. Here, we defined the following matrix why considering the unit vector from the target node to AN direction as:

$$A = \begin{bmatrix} \frac{(x_2^G - x_u)}{r_2^G} & \frac{(y_2^G - x_u)}{r_2^G} & \frac{(z_2^G - z_u)}{r_2^G} & 1 \\ \frac{(x_3^G - x_u)}{r_3^G} & \frac{(y_3^G - y_u)}{r_3^G} & \frac{(z_3^G - z_u)}{r_3^G} & 1 \\ \vdots & \vdots & \vdots & \vdots \end{bmatrix} \quad (21)$$

Let the matrix h be

$$h = (A^T A)^{-1} \quad (22)$$

Then, PDOP can be expressed as follows:

$$PDOP = \sqrt{h_{11} + h_{22} + h_{33}} \quad (23)$$

The smaller the value of PDOP, the better is AN arrangement with higher positioning accuracy. Therefore, to achieve high positioning accuracy, the target node will be at the origin and the receiver ANs centered on the hemisphere. Since it is difficult to find a combination that minimizes (23). The virtual particles should be spread on the hemisphere and randomly add particles. Take out and compare the respective PDOPs to find the optimum placement.

C) Positioning Error Model

The primary performance condition in a ranging system is its accuracy, commonly characterized by the root mean square error (RMSE). RMSE indicates the difference between the real and estimated position of a target node. It can be calculated by expressing the estimated point in the latitude longitude-height (LLH) coordinates using the origin's true target node position. The height error is given by

$$H_r = \sqrt{L_a^2 + L_o^2} \quad (24)$$

Where L_a and L_o are the latitude and Longitude errors respectively. Next, we calculate the RMSE as:

$$H_{RMSE} = \sqrt{L_{o_{RMSE}}^2 + L_{a_{RMSE}}^2}$$

Where $L_{o_{RMSE}}$ and $L_{a_{RMSE}}$ is the latitude and longitude RMSE error respectively.

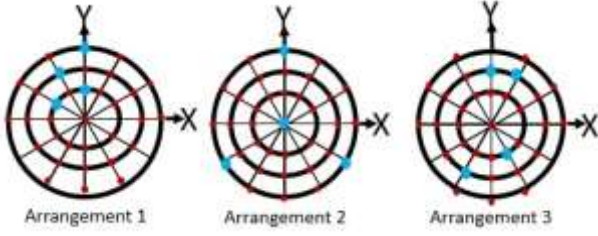


Fig .3. AN Optimal Placement and Random Placement

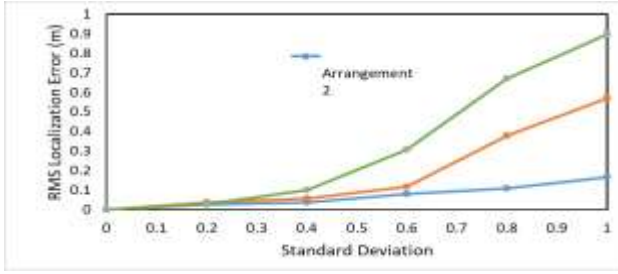


Fig.4. Difference in positioning error due to anchor node arrangement.

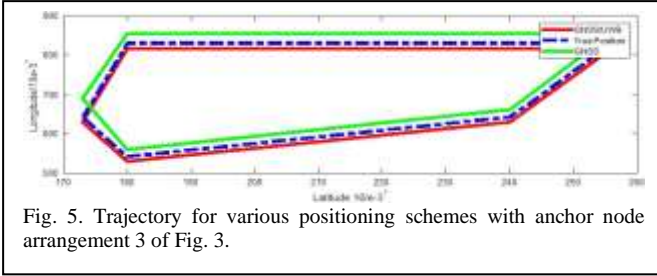


Fig. 5. Trajectory for various positioning schemes with anchor node arrangement 3 of Fig. 3.

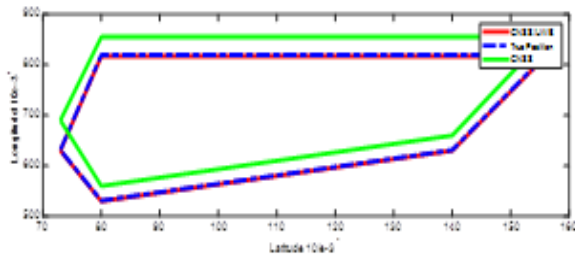


Fig. 6. Optimized GNSS/UWB Positioning with AN Placement as in Arrangement 2

D) Improvement Rate Analysis

To analysis the improvement rate of our proposed model, we calculate the improvement rate as follows:

$$\text{Improvement rate} = \left(\frac{RMSE_{\text{integrated}}}{RMSE_{\text{non-integrated}}} \right) \times 100 \quad (25)$$

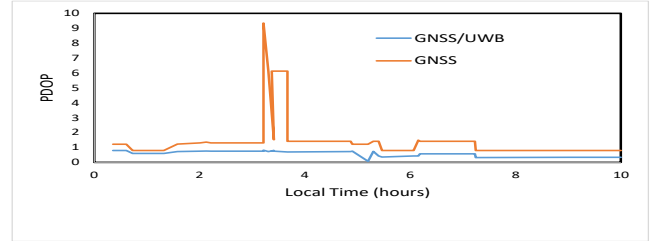


Fig.8. PDOP for ANs positioning as in arrangements 2 and 3 of Fig. 3 above.

B. Modeling Algorithm

Time slot 0 is the initial distribution

$X^{*(i)}_k$ is the estimate

1. For each particle $i = 1, 2, \dots, N_p$, sample the initial state $\rho X^{N(i)}_{x_0}$ from the initial distribution $\rho(X_0^{N(i)})$ and the different error variances.
2. Calculate and normalized the weights
3. For time slot $k = 1, 2, \dots$ do
4. Use the important distribution to sample the particles of time slot k $\rho X_k^{N(i)}(m) \approx q(X^{N(i)} \{X^{N(i)}_{k-1}\})$
5. In our simulations, we model the Ionospheric, PDOP, (23) RMS error as in (24) and (25), we also assumed that other errors model as in [11].
6. Average $\sum e$ over the number of Monte Carlo iterations. It this number is sufficiently high, and then a lower bound on the performance with any GNSS/UWB geometry is achieve.
7. Calculate the weights:

$$\omega_{p,k}^{N(i)}(m) \propto \rho(\xi_{G,k}^{(i)}, X^{*N(i)}_{k-1}, \xi_k^{N(i)} | X_k^{N(i)})$$

8. Normalize the weights:

$$\omega_{p,k}^{N(i)}(m) = \omega_{p,k}^{N(i)}(m) / \sum_{m=1}^{N_p} \omega_{p,k}^{N(i)}(m)$$

9. Resample and update the set of all the particles $\rho X_k^{N(i)}(m)$ then the weights become:

$$\omega_{p,k}^{N(i)}(m) = \frac{i}{N_p}$$

10. Project the particles to the $X^{*(i)}_k$ dimension, such that the new marginal particles are $\rho X_k^{(i)}(m)$. Then, the integrated state become:

$$X^{*(i)}_k = \frac{i}{N_p} \sum_{m=1}^{N_p} \rho X_k^{(i)}(m)$$

11. End for

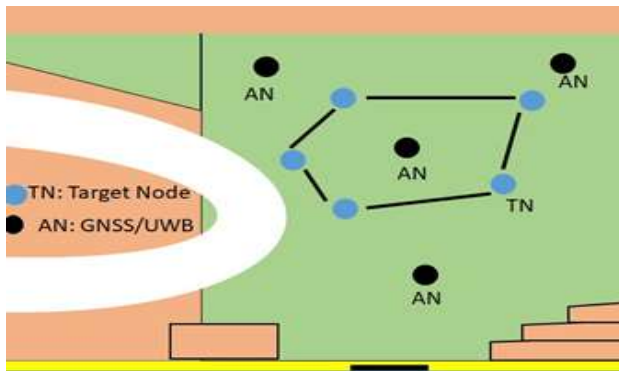


Fig.7. The target node will Stop on the blue dots and travel along the trajectory. The blue dots designate positions that have been surveyed.

IV. SIMULATION AND DISCUSSIONS

To test our proposed land survey method, we have carried out computer simulation within a challenging mixed environment, combining UWB and GNSS readings using a particle filter. We assume that all the GNSS systems have, on average, a similar geometry configuration of all the available navigation satellites (Nsv) satellites per design. The number of particles is 1000, the number of UWB is 4, the field is 100x100x100m, and the standard deviation of moving error is 0.5m.

In our simulation, four GNSS/UWB receivers were placed, as shown in fig.2 to cover the environment under analysis. During the simulation, data were simultaneously collected from the GNSS/UWB receivers and sampled using a particle filter to determine the anchor node position. It moves from one point to the other, collecting digital land points. In this analysis, we compare three different situations;

- 1) Analysis the positioning accuracy of GNSS/UWB and GNSS only environment.
- 2) Time taking by the target node using GNSS only and GNSS/UWB to determine its position.
- 3) A mixed environment with anchor nodes positions according to arrange arrangement 2 and arrangement 3 of Fig. 3.

The optimal positioning arrangement in Fig. 4 exiting at the origin is arrangement 2 with three ANs placed at the vertices of an equilateral triangle on the ground and the other placed at the zenith. Fig. 5 shows the target node trajectory in hostile conditions compared with two different solutions and with an anchor node position in arrangement 3 of Fig. 3. In the figure, the green and red lines show the difference between augmenting GNSS with and without UWB measurements, and the blue lines show the actual position of the target node. Fig. 5 equally indicates that the GNSS/UWB is more accurate than the GNSS-only solution. Fig. 6 shows the optimum placement of the anchor node as in arrangement 2 of Fig. 3. The figure shows that anchor node placement significantly affects positioning accuracy. In Fig. 7, blue dots designate locations where the target node is stopped along the trajectory, and the black dots represent anchor node placement. The Position Dilution of Precision (PDOP) solution in Fig. 8 shows that

GNSS/UWB ranges have the lowest PDOP values compared to GNSS only solution. Also, about 3, GNSS spikes up to 9, while the solution with GNSS/UWB does not observe such a dramatic increase. It can be attributed to the fact that the target node was in the densest environment. However, GNSS/UWB could weather this obstruction, and our proposed GNSS/UWB gives a stronger geometric strength on positioning accuracy.

V. CONCLUSION

This paper has implemented and evaluated a probabilistic framework for a land survey that merges different sensory sources. Based on the particle filter, our approach considers UWB, GNSS, and the combination of both technologies to reliably estimate a target node that moves from one point to the other, collecting digital land points in outdoor scenarios. Because UWB signals have characteristics that enable them to range accurately in high multipath and indoor conditions, its combination with GNSS is both beneficial and complimentary. The RMS error for the coordinate determination was 0.002 m, 0.004 m, 0.013 m for the northern, eastern, and height, respectively. Our proposed method performed much better, with 91% of the reliability. Also, it considerably reduced systematic errors and allowed all gross errors to be eliminated; however, this combination resulted in obtaining reliable coordinates with millimeters accuracy. Our proposed method permits a target node to rapidly and accurately collect the coordinates of a point. Results from computer simulation have been presented, proving the suitability of the proposed approach for land surveys.

REFERENCES

- [1] Da Bing Yaung, Wen Xin Zhang, Qing Yao, "Research of Mining Subsided Land Reclamation System based on GIS", *Metal Mine*, vol 10, 2011.
- [2] Bosy, Jarosław and, Artur Oruba, Marchin Leonczyk "ASG-EUPOS densification of EUREF Permanent Network on the territory of Poland", *Reports on Geodesy*, pp. 105–111, Jan 2008.
- [3] Bakula, Mieczysław and Oszczak, Stanisław and PelcMieczkowska, Renata, "Performance of RTK positioning in forest conditions: Case study", *Journal of Surveying Engineering*, vol 135, number 3, pp 125–130, 2009, *American Society of Civil Engineers*
- [4] Næsset, Erik and Gjevestad, Jon Glenn, "Performance of GPS precise point positioning under conifer forest canopies", *Photogrammetric Engineering & Remote Sensing*, vol. 74, No. 5, pp 661–668, 2008, *American Society for Photogrammetry and Remote Sensing*
- [5] Naesset, Erlk, "Effects of differential single-and dual-frequency GPS and GLONASS observations on point accuracy under forest canopies", *Photogrammetric engineering and remote sensing*, vol 67, number 9, pp 1021–1026, 2001, *ASPRS AMERICAN SOCIETY FOR PHOTOGRAMMETRY AND*
- [6] Hasegawa, Hisashi and Yoshimura, Tetsuhiko, "Application of dual-frequency GPS receivers for static surveying under tree canopies", *Journal of Forest Research*, Vol. 8, No. 2, pp 0103–0110, 2003, *Springer*

- [7] Valbuena, Ruben and Mauro, Francisco and Su´arez, R Rodr´ıguezSolano and Manzanera, JA, “Accuracy and precision of GPS receivers under forest canopies in a mountainous environment”, *Spanish Journal of Agricultural Research*, number 4, pp 1047–1057, 2010, *Instituto Nacional de Investigacio´n y Tecnologıa Agraria y Alimentaria (INIA)*
- [8] Edson, Curtis and Wing, Michael G, “Tree location measurement accuracy with a mapping-grade GPS receiver under forest canopy”, *Forest Science*, vol 58, number 6, pp 567–576, 2012, *Oxford University Press*.
- [9] Pirti, Atinc, and Gum˘us, Kutalmis, and Erkaya, Halil and Hos˘bas,˘ Ramazan Gursel, ”Evaluating repeatability of RTK GPS/GLONASS” near/under forest environment”, *Croatian Journal of Forest Engineering: Journal for Theory and Application of Forestry Engineering*, vol 31, number 1, pp 23–33, 2010, *Sumarski fakultet Sveuc˘ilis˘ta u Zagrebu˘*
- [10] Mieczysław Bakula, Przemysław, and Rafał ka˘zmierzak,˘ ”Reliable technology of centimeter GPS/GLONASS surveying in forest environments”, *IEEE Transactions on Geoscience and Remote Sensing*, vol 53, number 2, pp 1029–1038, 2014
- [11] Kinugasa, Natsuki and Takahashi, Fujinobu and Kohno, Ryuji, “Mitigation of Ionospheric Effect on Multi-GNSS Positioning with Ionosphere Delay Estimation Using Single-Frequency Measurements of Selected Satellites”, *Journal of Aeronautics, Astronautics and Aviation*, vol 49, number 2, pp 93–100, 2017.
- [12] Yedukondalu, Kamatham and Sarma, Achanta Dattatreya and Vemuri, Satya Srinivas “Estimation and mitigation of GPS multipath interference using adaptive filtering”, *Progress in Electromagnetics Research*, vol 21, pp 133–148, year 2011 *EMW Publishing*
- [13] Misra, Pratap and Enge, Per, “Global Positioning System: signals, measurements and performance second edition”, *Global Positioning System: Signals, Measurements and Performance Second Editions*, vol 206, 2006.
- [14] Seeber, Gunter, “Satellite Geodesy 2nd completely revised and” extended edition”, 2003, *Walter de Gruyter GmbH & Co. KG*.
- [15] Wanninger, Lambert and May, Manja, “Carrier phase multipath calibration of GPS reference stations”, *Proceedings of the 13th International Technical Meeting of the Satellite Division of The Institute of Navigation (ION GPS 2000)*, pp 132–144, 2000.
- [16] Dow, John M and Neilan, Ruth E and Rizos, “The international GNSS service in a changing landscape of global navigation satellite systems”, *Journal of geodesy*, vol 83, number 3-4, pp 191–198, 2009, *Springer*.
- [17] Reed, Jeffrey reed2005introduction, “Introduction to ultrawideband communication systems”, 2005, *Prentice Hall Press*.
- [18] Hoffman, J Randy, “Measurements to determine potential interference to GPS receivers from ultrawideband transmission systems”, 2001, *ITS*
- [19] Gonzalez, J and Blanco, JL and Galindo, C and Ortiz-de-Galisteo, A and Fernandez-Madrigal, JA and Moreno, FA and Martinez,˘JL, ”Combination of UWB and GPS for indoor-outdoor vehicle localization”, *2007 IEEE International Symposium on Intelligent Signal Processing*, pp 1–6, 2007.
- [20] Tan, Kian Meng and Law, Choi Look tan2007gps, title=GPS and UWB integration for indoor positioning, *2007 6th International Conference on Information, Communications & Signal Processing*, pp 1–5, 2007, *IEEE*.
- [21] Chiu, David S and MacGougan, Glenn and O’Keefe, “UWB assisted GPS RTK in hostile environments”, *Proceedings of the ION NTM*, 2008
- [22] Nur, Khalid and Feng, Shaojun and Ling, Cong and Ochieng, Washington, “Integration of GPS with a WiFi high accuracy ranging functionality”, *Geo-spatial Information Science*, vol 16, n0 3, pp 155– 168, 2013.
- [23] Parkinson, Bradford W and Enge, Per and Axelrad, Penina and Spilker Jr, James J, “Global positioning system: Theory and applications, Volume II”, 1996, *American Institute of Aeronautics and Astronautics*
- [24] Gustafsson, Fredrik and Gunnarsson, Fredrik, “Mobile positioning using wireless networks: possibilities and fundamental limitations based on available wireless network measurements”, *IEEE Signal processing magazine*, vol. 22, no. 4, pp 41–53, 2005.
- [25] Qi, Yihong and Kobayashi, Hisashi and Suda, Hirohito, “Analysis of wireless geolocation in a non-line-of-sight environment”, *IEEE Transactions on wireless communications*, vol. 5, no. 3, pp 672–681, 2006.
- [26] Weiss, Anthony J, ”Direct position determination of narrowband radio frequency transmitters”, *IEEE signal processing letters*, vol, 11, no 5, pp 513–516, 2004,
- [27] Gezici, Sinan and Poor, H Vincent, “Position estimation via ultrawide-band signals”, *Proceedings of the IEEE*, vol. 97, no. 2, pp 386–403, 2009, *IEEE*.
- [28] ,Lazzari, Fabrizio and Buffi, Alice and Nepa, Paolo and Lazzari, Sandro, ”Numerical investigation of an UWB localization technique for unmanned aerial vehicles in outdoor scenarios”, *IEEE Sensors Journal* vol 17, no 9, pp 2896–2903, 2017, *IEEE*.
- [29] Doucet, Arnaud and De Freitas, Nando and Gordon, Neil, “An introduction to sequential Monte Carlo methods”, pp 3–14, 2001, *Springer*.
- [30] Siciliano, Bruno and Khatib, Oussama, “Springer handbook of robotics”, 2016, *Springer*.
- [31] Ristic, Branko and Arulampalam, Sanjeev and Gordon, Neil, “Beyond the Kalman filter: Particle filters for tracking applications”, vol 685, 2004, *Artech house Boston*
- [32] Arulampalam, M Sanjeev and Maskell, Simon and Gordon, Neil and Clapp, Tim, “A tutorial on particle filters for online nonlinear/non-Gaussian Bayesian tracking”, *IEEE Transactions on signal processing*, vol. 50, no. 2, pp. 174–188, 2002.

Ngye Antoinette Agwa received a bachelor’s and master’s degree in Information and communication technology from the Department of Telecommunication, Information and Communication Technology (TICT), Faculty of Industrial Engineering, University of Douala, Cameroon, in 2012 and 2014 respectively. Since 2018, Antoinette has been a Ph.D. student in the Graduate School of Engineering Science, Yokohama National University, Japan. Since 2017, Antoinette has been an Assistant Lecturer with the Department of Computer Engineering, Faculty of Engineering and Technology, University of Buea, Cameroon. Her research areas of interest are cryptography, Geography information Security Ultra Wide Band, and Global Navigation Satellite System. Since 2020, she has been a student member of IEICE.

Takumi Kobayashi received the B.S. and M.S. degrees in Engineering from Musashi Institute of Technology in 2011 and Tokyo City University in 2013 respectively. Kobayashi received Ph.D degree in Engineering from Yokohama National University in 2016. Currently, Kobayashi is working with the Graduate School of Science and Engineering in Yokohama National University. His research interest includes UWB communications, medical information communication technology and human body communication. Dr. is a member of IEICE and IEEE EMBS, and a member of JSMBE.

Chika Sugimoto (M'11) received the B.S. degree in engineering the M.S. and Ph.D. degrees in environment from the University of Tokyo. From 2006 to 2010, Chika was an Assistant Professor with the Graduate School of Frontier Sciences, University of Tokyo. Since 2010, she has been an Associate Professor with the Faculty of Engineering, Yokohama National University. She is a member of IEICE and IEEE EMBS.

Ryuji Kohno Ryuji Kohno (F'12) received the Ph.D. degree from the Dept. Elec. Eng., University of Tokyo in 1984. Since 1998, he has been a Professor with Yokohama National Univ. From 1984 to 1985, he was a Visiting Scientist in the Dept. Elec. Eng., Univ. of Toronto. Since 2007, he has been a Finnish Distinguished Professor with the Univ. of Oulu, Finland. He was also a Director with Sony CSL/ATL during 1998- 2002, a Director with the UWB Technical Institute, and a program coordinator with the Medical ICT Institute of the NICT during 2002-2011. Since 2012, he has been the CEO with the Univ. of Oulu Research Institute Japan - CWC-Nippon Inc. Ltd. He was a Principal Leader of MEXT 21st century and Global COE programs during 2002-2007 and 2008-2013, respectively. Since 2003, he has been a Director with the Medical ICT Center, YNU. Since 2006, he has also been an Associate Member of the Science Council of Japan. He is IEICE and IEEE Fellows. He was elected a BoG Member of the IEEE Information Theory Society in 2000, 2002, and 2006. He received the IEICE Greatest Contribution Award and NTT DoCoMo Mobile Science Award in 1999 and 2002, respectively.